Enhanced charge carrier injection in heterojunction organic field-effect transistor by inserting an MoO_3 buffer layer*

Yu Xin-Ge(于欣格), Yu Jun-Sheng (于军胜)†, Huang Wei(黄 伟), and Zeng Hong-Juan(曾红娟)

State Key Laboratory of Electronic Thin Films and Integrated Devices, School of Optoelectronic Information, University of Electronic Science and Technology of China, Chengdu 610054, *China*

(Received 18 April 2012; revised manuscript received 8 May 2012)

A top-contact organic field-effect transistor (OFET) is fabricated by adopting a pentacene/1,1′-bis(di-4-tolylaminophenyl) cyclohexane (TAPC) heterojunction structure and inserting an MoO_3 buffer layer between the TAPC organic semiconductor layer and the source/drain electrode. The performances of the heterojunction OFET, including output current, field-effect mobility, and threshed voltage, are all significantly improved by introducing the MoO_3 thin buffer layer. The performance improvement of the modified heterojunction OFET is attributed to a better contact formed at the Au/TAPC interface due to the MoO_3 thin buffer layer, thereby leading to a remarkable reduction of the contact resistance at the metal/organic interface.

Keywords: organic field-effect transistor (OFET), MoO_3 buffer layer, heterojunction structure, contact resistance

PACS: 73.40.Cg, 73.61.Ph, 73.61.Wp, 85.30.Tv **DOI:** 10.1088/1674-1056/21/11/117307

1. Introduction

Organic field-effect transistors (OFETs) have attracted a great deal of attention because of their advantages, such as being light weight and flexible, and various applications, such as organic display, radio frequency identification tags, and sensors.[1−5] However, compared with inorganic Si-based transistors, the charge carrier mobility of OFET is still too low. In the last several years, the performance of OFET has been improved significantly by developing promising functional materials[6−9] and creating optimized device structures.[10−12] Among many advanced OFET structures, the organic semiconductor heterojunction is an effective architecture to improve the performance of OFET,[6,13,14] which has also been extensively utilized in organic light-emitting diodes (OLEDs)[15,16] and organic photovoltaic cells (OSCs).[17,18] The reason is that the heterojunction structure in OFET possesses the advantage of increasing the conductivity of the active layer, morphological matching between different organic films, and manipulating the interface molecular level alignment.

Meanwhile, the contact problem between the organic film and source/drain (S/D) electrodes is crucial, which restricts the development of OFETs, since an inevitable injection barrier always exists between the organic semiconductor and S/D electrodes.[19−21] Therefore, a buffer layer, e.g. MoO_3, Bphen, C_{60}, has been inserted between the organic film and S/D electrodes to reduce the injection barrier.[22−25] Similarly, in heterojunction OFETs, especially top-contact OFETs with a heterojunction structure, the injection barrier still exists between S/D electrodes and the organic layer. However, most research on heterojunction OFETs has focused mainly on the interfacial properties of the two active layers, while the contact behaviour of the organic/electrodes in the heterojunction OFET has received less attention. Thus, introducing a thin buffer layer at the interface of organic/electrodes could be helpful for further improving the performance of the heterojunction OFET.

In this work, a heterojunction architecture comprised of a pentacene film and a 1,1′-bis(di-4-tolyla-

*Project supported by the National Natural Science Foundation of China (Grant Nos. 61071026 and 61177032), the Science Fund for Creative Research Groups of the National Natural Science Foundation of China (Grant No. 61021061), the Fundamental Research Fund for the Central Universities of Misistry of Education of China (Grant No. ZYGX2010Z004), and the Specialized Research Fund for the Doctoral Program of Higher Education of China (Grant No. 20090185110020).

†Corresponding author. E-mail: jsyu@uestc.edu.cn

© 2012 Chinese Physical Society and IOP Publishing Ltd

minophenyl) cyclohexane (TAPC) film is used as the active layer of the OFET. Meanwhile, a thin MoO_3 buffer layer is inserted between the S/D electrode and the TAPC film to reduce the charge injection barrier. The electrical properties of the heterojunction OFET are characterized and investigated. The reason for the performance improvement is analysed by using the organic/metal interfacial properties and the contact resistance.

2. Experiment

As shown in Fig. 1, top-contact heterojunction OFETs were fabricated according to the following procedure. The indium tin oxide (ITO) coated glasses were used as gate electrodes and substrates, respectively. A 520 nm thick PMMA dielectric layer was spin-coated onto the transistor and baked on a hot plate at 150 °C for 1 h to serve as the gate insulator with a unit capacitance of 5.1 nF/cm^2. The 25 nm thick pentacene and 15 nm thick TAPC were deposited in succession under a vacuum of less than 2×10^{-4} Pa at the rates of 0.2 Å/s and 0.5 Å/s, respectively. Subsequently, a 5 nm thick MoO_3 buffer layer was deposited on the TAPC film and patterned with a shadow mask. The source and the drain electrodes of gold (Au) were thermally evaporated on the MoO_3 buffer layer finally. The width and the length of the channel were 5 mm and 50 μm to 200 μm, respectively. For comparison, the heterojunction OFET without the MoO_3 buffer layer, pentacene OFETs with and without MoO_3 buffer layers were also fabricated in the same way. The electrical characteristics were measured with a Keithley 4200 programmable bias-current source in air under ambient circumstances.

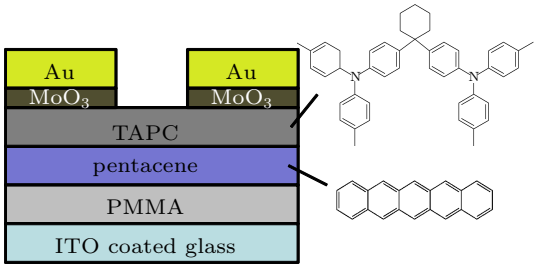


Fig. 1. (colour online) Architecture of the heterojunction OFET, and the chemical structures of TAPC and pentacene in this study.

3. Results and discussion

Figures 2(a)–2(h) show the typical output and transfer characteristics of the OFETs with four structures, i.e., the single pentacene layer OFET without any buffer layer (structure A), the pentacene OFET with an MoO_3 buffer layer (structure B), the pentacene/TAPC heterojunction OFET without any buffer layer (structure C), and the pentacene/TAPC heterojunction OFET with an MoO_3 buffer layer (structure D). These devices all exhibit high currents with good saturation behaviour and conform well to the conventional FET models in both the linear and the saturation regimes. Figures 2(a) and 2(b) show the characteristics of the OFET with structure A. When the gate voltage V_{GS} is maintained at −40 V and the drain voltage is swept from 0 to −40 V, the saturation current I_{SD} is found to be 138 μA. From the $I_{SD}^{1/2} - V_{GS}$ curve, the extracted threshold voltage (V_T) is about −11.5 V. Figures 2(c) and 2(d) show the characteristics of the OFET with structure B. It can be seen that the saturation current I_{SD} and V_T of this transistor show only a little improvement, and the corresponding reason is that the performance of the OFET could be obviously enhanced by optimizing the Au S/D deposition rate, which has been demonstrated in our recent work,[26] and similar results have also been reported by other groups.[27,28] As indicated in Figs. 2(e) and 2(f), the heterojunction OFET with structure C has not only a high value of the threshold voltage (∼ −18 V), but also a lower value of I_{SD} than that of the single pentacene layer device (structure A). When an MoO_3 buffer layer is inserted between TAPC and Au, the OFET with structure D shows improvements on both I_{SD} and V_T, which are shown in Figs. 2(g) and 2(h), repectively. Meanwhile, the field-effect mobilities of the devices with different structures can be calculated in the saturation region using the following equation:

$$I_{DS} = (WC_i/2L)\mu(V_{GS} - V_T)^2, \qquad (1)$$

where C_i is the capacitance per unit area of an insulator, I_{DS} is the output current in the saturation region, and W and L are the channel width and length, respectively. From Eq. (1), the calculated field-effect mobilities of the pentacene OFETs (with structures A and B) are about 0.67 ∼ 0.68 cm^2/(V·s), while those of the devices with the heterojunction structure (structure C and D) are higher than 0.9 cm^2/(V·s). The higher mobility of the heterojunction OFET presents the conductivity of the heterojunction pentacene/TAPC film, which is much higher than that of the pentacene film. The extracted field-effect mobilities, saturation currents, as well as threshold voltages of these OFETs are listed in Table 1.

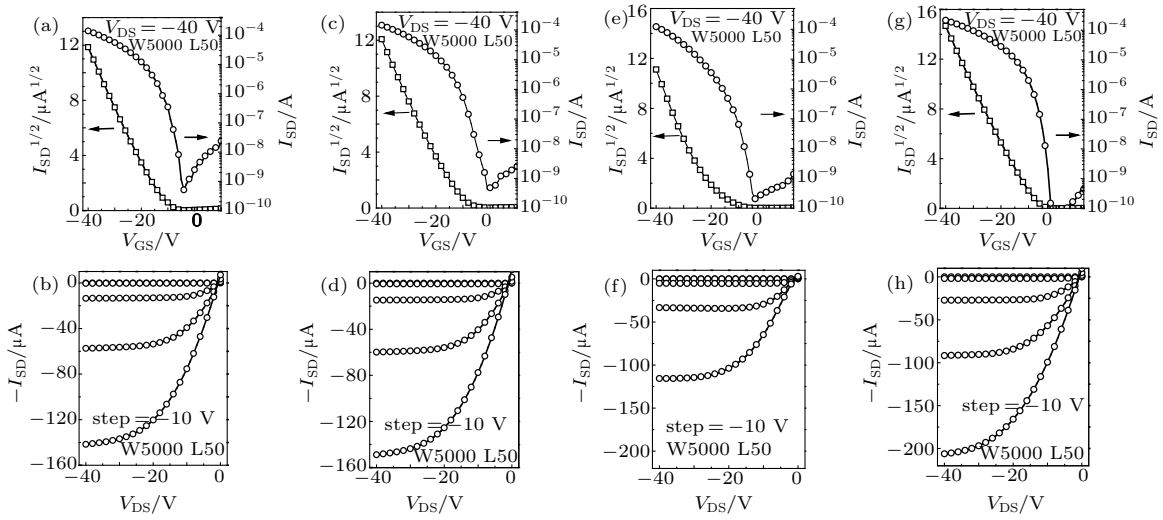


Fig. 2. Typical output $I_{DS} - V_{DS}$ and transfer $I_{DS} - V_{GS}$ curves of OFETs with different structures: structure A ((a), (b)), structure B((c),(d)), structure C((e),(f)), structure D ((g),(h)). The channel width and length are $W = 5$ mm and $L = 50$ μm for all the devices.

From Table 1, it can be clearly observed that V_T of the heterojunction OFET without any buffer layer presents the highest value among all the devices. While V_T of the heterojunction OFET with an MoO_3 buffer layer presents the lowest value, which is even lower than that of the pentacene OFET with an MoO_3 buffer. In addition, the saturation current of the heterojunction OFET with structure D is almost twice as high as that of the device with structure C. This result demonstrates the effectiveness of using an MoO_3 buffer layer in the heterojunction OFET for improving the contact behaviour, which in turn results in the improvement on the charge injection efficiency.[22]

Table 1. Values of saturation current I_{SD}, threshold voltage V_T, field-effect mobility μ of OFETs with structures A, B, C, and D.

Device	Saturation current/μA	Threshold voltage/V	Field-effect mobility /cm^2·V^{-1}·s^{-1}
Structure A	138	−11.5	0.67
Structure B	146	−11	0.68
Structure C	115	−18	0.93
Structure D	220	−9	0.91

In order to understand the reason for the improved performance after inserting an MoO_3 buffer layer in the heterojunction OFET, the interfacial properties are further investigated by analysing the energy level between S/D electrodes and TAPC organic film. In the previous work, it has been shown that the contact between the S/D electrode and the organic active layer can be improved significantly by inserting an MoO_3 buffer layer in the top-contact OFET.[22,29] Figure 3 shows the energy level diagrams of Au/TAPC and Au/MoO_3/TAPC in this work. In the heterojunction device without any buffer layer between the S/D electrode and the TAPC, a large injection barrier is formed when the Au electrode directly contacts TAPC film. The injection barrier is caused by two factors: a) the highest occupied molecular orbital (HOMO) of TAPC ∼ 5.5 eV, which is higher than that of the work function of Au ∼5.1 eV; b) the energy shift caused by the dipole formation effect at the interface of the metal/organic junction, which can be expressed by the following model:[30]

$$\begin{aligned}\varphi_{\text{real}} &= \varphi_{\text{ideal}} + \Delta \\ &= U(\text{HOMO} - \psi_{\text{metal}}) \cdot (\text{HOMO} - \psi_{\text{metal}}) \\ &\quad + \sum\nolimits_i \int_0^{\pi} \frac{N_i(\theta) P_i \cos\theta}{\varepsilon_r \varepsilon_0} \mathrm{d}\theta, \end{aligned} \tag{2}$$

where φ_{real} is the practical injection barrier height from the S/D electrode to the organic semiconductor; φ_{ideal} is the barrier height from the work function of the metal ψ_{metal} to the HOMO level of the organic semiconductor; $U(x)$ is the unit step function, and $U(x) = 0$, if $x < 0$, $U(x) = 1$, if $x \geq 0$; θ is the alignment angle between the dipole element and interface normal; N_i and P_i are the density and the moment of the dipole element type i, respectively. From Eq. (2), the φ_{real} from Au to TAPC is determined both by φ_{ideal} and the dipole formed at the metal/organic interface shown in Fig. 3(a). Therefore, by inserting a thin MoO_3 layer between the Au electrodes and the TAPC film, as shown in Fig. 3(b), the barrier height from Au to TAPC is modulated, and the dipole formation effect is mitigated,[23,30] resulting in a reduction

in the injection barrier. In addition, the MoO_3 buffer layer could also reduce the charge carrier traps at the organic/metal interface.[23,26,29,30] Therefore, the injection current increases effectively, and the V_T decreases from −18 V to −9 V. Moreover, the reason for this improvement can be further illuminated by the contact resistance based on the transfer line method, which could be helpful for scrutinizing the contact between Au and TAPC.

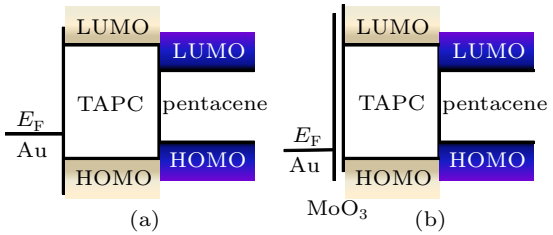


Fig. 3. (colour online) Energy level diagrams of the Au/TAPC interface (a) without and (b) with an thin MoO_3 buffer layer.

The values of contact resistance R_C of the OFET with various structures are calculated from by[19,26]

$$R_{\text{total}} = R_C + \frac{L}{W \cdot \mu \cdot C_i(V_{GS} - V_T)}, \qquad (3)$$

where R_{total} is the total resistance in the linear region of $I_{DS} - V_{DS}$ characteristics. As the channel width W is a constant, R_{total} can be treated as a function of the channel length L of the OFET. As a result, R_C can be extracted by giving $L = 0$ in Eq. (3). When the gate voltage is $V_{GS} = -40$ V and the drain-source voltage V_{DS} is in the linear region, the linear relationships between R_{total} and L of OFET with different structures can be derived from Fig. 4. Hence, the calculated contact resistance R_C shows little discrepancy in the pentacene OFET, corresponding to 0.038 MΩ for the device with structure A and 0.035 MΩ for the device with structure B. While in the heterojunction OFETs,

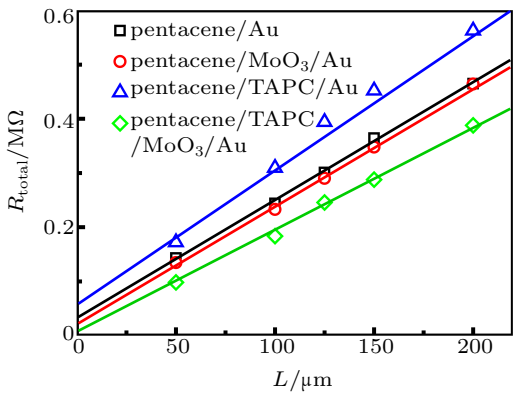


Fig. 4. (colour online) Transfer line method plots for various devices with different structures. The zero-intercept of the fitted lines determines the contact resistance R_C. The gate voltage is $V_{GS} = -40$ V.

R_C is reduced from 0.061 MΩ to 0.011 MΩ for the case where the thin MoO_3 buffer layer is inserted between the TAPC and Au electrodes, which is even lower than that of devices with structure B. Such results exhibit that the contact between the TAPC and Au electrodes is optimized by inserting the MoO_3 buffer layer.

4. Conclusions

In conclusion, by inserting a thin MoO_3 buffer layer between the TAPC and Au electrodes in TAPC/pentacene heterojunction OFETs, the performance of the heterojunction OFET, such as injection current and threshold voltage, can be greatly improved, The obvious improvement is attributed mainly to a reduction in the contact resistance at the organic/metal interface, which is of benefit to the charge carrier injection from the Au electrode to the TAPC film. Such a result suggests that the use of a buffer layer to reduce the contact resistance is an extremely promising technique in improving the performance of heterojunction OFETs, which is helpful for designing the architecture of heterojunction OFETs with improved performance.

References

[1] Rogers J A, Bao Z N, Baldwin K, Dodabalapur A, Crone B, Raju V R Kuck V, Katz H E, Amundson K, Ewing J and Drzaic P 2001 *Proc. Natl. Acad. Sci. U.S.A* **98** 4835

[2] Gelinck G H, Huitema H E A, van Veenendaal E, Cantatore E, Schrijnemakers L, Van Der Putten J B P H, Geuns T C T, Beenhakkers M, Giesbers J, Huisman B H, Meijer E J, Benito E M, Touwslager F J, Marsman A W, van Rens B J E and de Leeuw D M 2004 *Nat. Mater.* **3** 106

[3] Sekitani T, Zschieschang U, Klauk H and Someya T 2010 *Nat. Mater.* **12** 1015

[4] Lin P and Yan F 2012 *Adv. Mater.* **24** 34

[5] He Y D, Dong H L, Meng Q, Jiang L, Shao W, He L F and Hu W P 2011 *Adv. Mater.* **23** 5502

[6] Benning P J, Poirier D M, Ohno T R, Chen Y, Jost M B, Stepniak F, Kroll G H, Weaver J H, Fure J and Smalley R E 1992 *Phys. Rev.* B **45** 6899

[7] Podzorov V, Pudalov V M and Gershenson M E 2003 *Appl. Phys. Lett.* **82** 1739

[8] Ortiz R P, Herrera H, Blanco R, Huang H, Facchetti A, Marks T J, Zheng Y and Segura J L 2010 *J. Am. Chem. Soc.* **132** 8440

[9] Braga D, Campione M, Borghesi A and Horowitz G 2010 *Adv. Mater.* **22** 424

[10] Wang J, Wang H B, Yan X J, Huang H C, Jin D, Shi J W, Tang Y H and Yan D H 2006 *Adv. Funct. Mater.* **16** 824

[11] Hwang D K, Hernandez C F, Kim J, Potscavage Jr W J, Kim S J and Kippelen B 2011 *Adv. Mater.* **23** 1293

[12] Jeon J, Tee B C K, Murmann B and Bao Z N 2012 *Appl. Phys. Lett.* **100** 043301

[13] Wang H B Liu Z T, Lo M F, Ng T W, Lee C S, Yan D H and Lee S T 2010 *J. Appl. Phys.* **107** 024510

[14] Kim F S, Ahmed E, Subramaniyan S and Jenekhe S A 2010 *ACS Appl. Mater. Interfaces* **2** 2974

[15] Yang R Q, Tian R Y, Yan J G, Zhang Y, Yang J, Hou Q, Yang W, Zhang C and Cao Y 2005 *Macromolecules* **38** 244

[16] Zhao J, Yu J S, Hu X, Hou M H and Jiang Y D 2012 *Thin Solid Films* **520** 4003

[17] Huang J, Yu J S, Wang W and Jiang Y D 2011 *Appl. Phys. Lett.* **98** 023301

[18] Wang N N, Yu J S, Zang Y, Huang J and Jiang Y D 2010 *Sol. Energy Mater. Sol. Cells* **94** 263

[19] Yu X G, Yu J S, Zhou J L, Huang J and Jiang Y D 2011 *Appl. Phys. Lett.* **99** 063306

[20] Darmawan P, Minari T, Kumatani A, Li Y and Liu C 2012 *Appl. Phys. Lett.* **100** 013303

[21] Yu X G, Yu J S, Huang W, Zhang L and Zeng H J 2012 *AIP Advances* **2** 022113

[22] Wang Z, Alam M W, Lou Y, Naka S and Okada H 2012 *Appl. Phys. Lett.* **100** 043302

[23] Chu C W, Li S H, Chen C W, Shrotriya V and Yang Y 2005 *Appl. Phys. Lett.* **87** 193508

[24] Zhou J L, Yu J S, Yu X G and Cai X Y 2012 *Chin. Phys.* B **21** 027305

[25] Sun Q J, Xu Z, Zhao S L, Zhang F J and Gao L Y 2011 *Chin. Phys.* B **20** 017306

[26] Yu X G, Yu J S, Zhou J L and Jiang Y D 2012 *Synth. Met.* **162** 936

[27] Park J, Kang J M, Kim D W and Choi J S 2010 *Thin Solid Films* **518** 6232

[28] Zhang X H, Domercq B and Kippelen B 2009 *Synth. Met.* **159** 2371

[29] Sun Q J, Xu Z, Zhao S L, Zhang F J, Gao L Y and Wang Y S 2010 *Synth. Met.* **160** 2239

[30] Liu Z H, Kobayashi M, Paul B C, Bao Z N and Nishi Y 2010 *Phys. Rev.* B **82** 035311